

**Dynamic Mechanical and Impact Property
Correlation of Nanoclay and Graphite Platelet
Reinforced Vinyl Ester Nanocomposites**

INTRODUCTION

In the past decade several polymer composites have been developed to improve modulus, strength, fatigue, corrosion mitigation, durability, flammability, and visco-elastic response. It is reported that mechanical and thermo-mechanical properties of composites are vastly improved by reinforcing the polymer with nano-sized particles rather than micron-sized particles of the same material [1]. One of the reasons attributed to this is fewer defects in the filler particle at the nano level as compared to micro or macro level [2]. Further, many important chemical and physical interactions are governed by surfaces and surface properties [3]. Hence, nanoreinforcements having very high surface to volume ratio exhibit substantially different composite properties.

These new class of composites are increasingly being studied for their application in structures such as spacecrafts, airplanes, warships etc. which require high stiffness-to-weight ratio along with high damping. Nanoclay [4-7] and graphite platelets [8-12] are some of the nano scale inclusions proposed as filler materials showing promise for structural applications, and have been investigated in this work for naval ships and homeland security applications. It is well known and documented that stress state in composites could be multi-axial and non-uniform even for a uniaxial loading due to complex interaction between the fiber and matrix. Hence, a detailed study into the dynamic behavior and the principles guiding them is a must before putting these nanocomposites in use. It includes understanding the elastic and fracture properties as well as interaction between fiber/matrix interface.

Structural materials subjected to dynamic loading should have high stiffness along with high damping. Further, they should have high storage modulus to enhance the ability to absorb energy before failure as well as high loss modulus to dissipate the energy. High damping or loss factor ($\tan \delta$) expressed as the ratio of loss modulus to the storage modulus, is also desirable to avoid catastrophic failure.

The objective of this work is to study the impact and dynamic properties of nanoclay/ vinyl ester and graphite platelet/ vinyl ester nanocomposites with 1.25 and 2.5 wt percent nano reinforcements and comparison with pure polymer. These nanocomposites are proposed as face plates of sandwich composite structure with fire-resistant foam layered in between to enhance the energy absorption along with optimal flexural rigidity, vibration damping and reduced flammability. This new class of material is expected to make the structure blast/shock/impact resistant with reduced weight for naval ships and homeland security applications.

EXPERIMENTS

Specimen Preparation

For this research, Derakane 411-350 vinyl ester thermoset plates of dimension 280 mm x 280 mm x 10 mm (10" x 10" x 0.39") were manufactured at Michigan State University with 1.25 and 2.5 wt percent of cloisite 30B nanoclay and exfoliated graphite nanoplatelets (xGnP). High viscosity of vinyl ester resin restricted the higher percentage of nano reinforcement due to the problems with removal of entrapped air and improper mixing.

Dynamic mechanical analysis was performed in single cantilever deformation mode with fixed-fixed boundary condition using a clamp having a span of 17.5 mm (0.69"). Prismatic samples with nominal dimension of 10.0 mm width x 1.6 mm thk. (0.39" x 0.06") were milled

from the manufacturer supplied plates and cut to a length of approximately 30 mm (1.18”) to provide sufficient overhang for clamping. It is to be noted that in all the samples, thickness of supplied plate (10 mm) was used as width for the DMA sample. Two samples were tested from each configuration.

Low-velocity impact tests were performed in flexure mode using simply supported fixture with a span of 95.25 mm (3.75”). Impact samples were milled to the dimensions of 127 x 10.0 x 12.7 mm (5” x 0.39” x 0.5”), as per ASTM D-6110-06 [13] test requirements. Five samples were tested from each configuration with and without notch. The notch, where applicable, was cut by specially made milling cutter with an angle of 45° and a depth of 2.54 mm (0.1”) from top of plate, maintaining a dimension of 10.16 ± 0.05 mm ($0.400” \pm 0.002”$) for thickness under notch. It is to be noted that thickness of the specified plate (10 mm) was used as width for impact sample.

Dynamic Mechanical Analysis

Dynamic mechanical analyzer (DMA) is used to characterize the dynamic properties of material as a function of temperature and frequency. It is a powerful technique used to characterize the storage modulus, loss modulus, damping and glass transition temperature of visco-elastic materials by subjecting small samples to an oscillatory load under a controlled temperature program. Material under testing is vibrated in flexure at varying temperature; and force and amplitude are recorded to obtain the dynamic properties.

DMA tests were performed in accordance with ASTM D4065-01: “Standard Practice for Plastics: Dynamic Mechanical Properties: Determination and Report Procedures” [14] using model Q800 DMA (TA Instruments, USA) and recommendations of the machine manufacturer [15, 16]. The schematic of the machine is shown in Figure 1.

DMA Q800 is a controlled stress with a combined motor and transducer (CMT) machine in which the motor applies a force and displacement sensors measure strain. Force and amplitude are the raw signals recorded by the machine. Stiffness is calculated directly from force and amplitude and modulus is calculated by multiplying the stiffness by an appropriate geometry factor. The geometry factor for a single-cantilever clamp is calculated by [15]:

$$GF = \frac{1}{F} \left[\frac{L^3}{12I} + 2S(1+\nu) \frac{L}{A} \right] \quad (1)$$

where:

L = sample span length of one side (mm)

A = sample cross sectional area (mm²)

I = geometric moment (mm⁴) = (bh³/12)

h = sample thickness (mm)

b = sample width (mm)

F = clamping factor (nominally 0.9)

S = shearing factor (nominally 1.5)

ν = Poisson’s ratio (nominally 0.44)

As can be seen from the formula, the geometry factor is an exponential function of span length and thickness. Hence, it is important that due care is taken in measurement of the samples. A digital vernier caliper with a least-count of 0.005 mm was used in this test, and the average of

width and thickness at five different locations was recorded. A variation of less than 0.03 mm was observed in the dimensions of the individual sample.

After several trial runs, single cantilever clamp was used for experiments. Three-point bend clamp was first tried because of the advantage of nullifying friction and clamping effects but stiffness of vinyl ester nanocomposites was dropping below working range of machine for larger sample required in three-point bend clamp.

Testing of all the specimens were done at a frequency of 1 Hz and displacement amplitude of 25 μm . Temperature range of -50°C to 150°C with a temperature ramp of 3°C per minute was used for characterization. Samples were clamped with a torque of 1.13 N-m (10 lb-in) and two samples were tested from each configuration.

Low-velocity Impact Test

Low-velocity impact tests were performed in a drop-weight instrumented impact test system (Dynatup Model 8250) and the test method used was comparable to that of ASTM D6110-06 [13]. The difference being that a drop-weight system was used instead of pendulum type machine recommended in the standard. Setup of machine is shown in Figure 2 and a schematic is shown in Figure 3.

Dimension of the samples were used as input in the Instron software for calculation of normalized-to- thickness (NTT) values of absorbed energy. For this purpose, all the dimensions except that of notch were measured using digital vernier caliper with least count of 0.01 mm (0.0005"). Notch dimensions of random specimens were verified on comparator for angle, depth and radius. In all other samples, notch depth was measured using vernier caliper and a straight edge. Straight edge was kept on top of the surface and depth was measured using inside jaws of vernier caliper with one jaw on straight edge and another on end of notch.

Specimens of dimensions as specified earlier were kept on a steel support fixture having central span (Dimension Span, Figure 3) of 95.25 mm (3.75") with notch (where applicable) facing down, simulating a simply supported beam configuration. These specimens were impacted with a steel charpy tup from a suitable drop height. It was ensured that the steel tup hits the specimen at the middle both lengthwise as well as widthwise by providing appropriate stoppers in the fixture.

After several trial runs, the cross head weight was set at 2.364 Kg (5.2 lbs) providing a total drop weight of 3.318 Kg (7.3 lbs) with a drop height of 177.8 mm (7"). Load range used for tests was standardized to 4.448 kN (1000 lbs.). Filter was set at 4 KHz and time for data collection was set to 20 mS. Velocity slowdown of less than 20% was observed in all the results.

RESULTS AND DISCUSSION

Figures 4 and 5 show typical outputs of storage modulus, loss modulus and loss factor as a function of temperature for pure vinyl ester and 2.5 wt percent graphite platelet/ vinyl ester nanocomposite. Figures 6 to 8 show the comparison of storage modulus, loss modulus and loss factor with respect to temperature for vinyl ester nanocomposites. Glass transition temperature reported here is from the peak of loss modulus, as per ASTM D4065-01 [13], and loss factor (damping) from peak of $\tan \delta$ curve. Note that these figures show the output of one sample, and the α transition has been used for reporting the peak $\tan \delta$ value. It is also to be noted that only

one distinct $\tan \delta$ peak was observed in case of the 2.5 wt. percent graphite platelet reinforced vinyl ester.

It is observed that storage modulus increases gradually with increase in nanoclay reinforcement in vinyl ester. However, 2.5 wt percent graphite platelet reinforcement shows significant improvement (approximately 30%) in storage modulus as compared to 1.25 wt percent reinforcement. Glass transition temperature and loss factor also showed an increase with increasing reinforcement for both nanoclay and graphite platelets.

Figures 9 and 10 show typical outputs of load (and energy) vs. deflection for low-velocity impact tests performed on two un-notched and notched samples of 2.5 wt. percent graphite platelet/vinyl ester nanocomposites. Figures 11 to 13 show the maximum load, total energy absorption up to failure, and normalized-to-thickness (NTT) total energy of pure vinyl ester and their nanocomposites.

Maximum load and total energy is shown to be increasing with increasing reinforcement of nanoclay as well as graphite platelet reinforcements in un-notched specimens while it decreased for all the notched specimens. Notch sensitivity shown with nanoreinforcement may be attributed to the interfacial stress transfer phenomenon noted by L. Roy Xu et. al. [18, 19] due to stress singularity at the fiber-matrix interface, and inefficient interfacial shear stress transfer in discontinuous fiber because of the high stiffness property mismatch.

Figures 14 to 18 show the correlation of total absorbed energy obtained from impact tests with respect to: storage modulus at room temperature; loss modulus at room temperature and at glass transition temperature; loss factor at peak of $\tan \delta$; and the glass transition temperature, obtained from the DMA tests. Figures also show the proportional variability in the output values using the square of the correlation coefficient, R^2 .

Results demonstrate that an increase in loss modulus at room temperature (Figure 15), and high loss factor peak (Figure 17) will most likely improve the impact energy absorption. However, the percentage increase is different for nanoclay and graphite platelet reinforcement, with nanoclay showing more sensitivity to loss modulus at room temperature. It is also observed that increase in loss modulus at the glass transition temperature (Figure 16), where cross-link molecular interaction of the resin plays a more important role in determining the material properties, reduces impact energy for nanoclay reinforcement while no direct correlation can be established for graphite platelet reinforcement. Storage modulus (Figure 14) and glass transition temperature (Figure 18) also show some correlation with the impact energy. This phenomenon is different from earlier experiments on sheet molding compound (SMC) glass resin composite formulations which showed poor correlation of impact properties with the dynamic mechanical properties [20]. Detailed studies using different matrices and reinforcement material are required to establish a relationship between the dynamic and impact properties.

CONCLUSIONS

From DMA experiments, storage modulus of graphite platelet reinforcement showed a greater improvement in storage modulus, loss modulus, and glass transition temperature as compared to nanoclay, where as nanoclay shows better improvement in loss factor as compared to graphite platelet reinforcement. On the other hand, nanoclay reinforcement shows better low-velocity impact resistance in terms of energy absorption and maximum load before failure. It is observed that for un-notched specimens, the energy absorption doubled when reinforced with 2.5

wt. percent Cloisite 30B nanoclay and graphite platelets. However, notched specimens showed a 50% decrease in energy absorption for 2.5 wt. percent nanoclay and a 75% decrease for 2.5 wt. percent graphite platelet reinforcement, suggesting their notch sensitivity.

An attempt was made to see if there is any correlation between impact properties and dynamic properties. Impact energy was observed to have some relationship with loss modulus at room temperature with different sensitivity for nanoclay and graphite platelet reinforcement as well as with loss factor. However, loss modulus at glass transition temperature showed poor correlation with impact energy for graphite platelet reinforcement.

ACKNOWLEDGEMENTS

The authors would like to acknowledge the support received from the Department of Civil Engineering at the University of Mississippi, and funding received under a subcontract from the Department of Homeland Security-sponsored Southeast Region Research Initiative (SERRI) at the Department of Energy's Oak Ridge National Laboratory. Support for this research by ONR Grant # N00014-07-1-1010, Office of Naval Research, Solid Mechanics Program (Dr. Yapa D.S. Rajapakse, Program Manager) is also acknowledged. The nano clay and graphite platelet / vinyl ester composite plates were manufactured by Dr. Larry Drzal's group at Michigan State University- Composite Materials and Structures Center.

REFERENCES

1. M. Sumita, Y. Tsukumo, K. Miyasaka, and K. Ishikawa. 1983. "Tensile yield stress of polypropylene composites filled with ultrafine particles" *Journal of Materials Science*, 18(1983): 1758-1764.
2. Fischer H. "Polymer nanocomposites: from fundamental research to specific applications" *Material Science and Engineering*; 23(2003):763:772
3. Hussain F., Hojjati M., Okamoto M. and Gorga R. E., "Polymer-matrix Nanocomposites, Processing, Manufacturing, and Application: An Overview" *Journal of Composite Materials*; 40(2006): 1511:1575.
4. Schmidt, D., Shah, D. and Giannelis, E.P. (2002). "New Advances in Polymer/Layered Silicate Nanocomposites", *Current Opinion in Solid State and Materials Science*, 6(3): 205–212
5. Ray, S.S. and Okamoto, M. (2003). "Polymer/layered Silicate Nanocomposite: A Review from Preparation to Processing", *Prog. Polymer Sci.*, 28: 1539–1641
6. Bhat G., Hegde R. R., Kamath M.G., and Deshpande B., "Nanoclay Reinforced Fibers and Nonwovens", *Journal of Engineered Fibers and Fabrics* 2008; 3(3): 22-34
7. Alexandre M., Dubois P., "Polymer-layered silicate nanocomposites: preparation, properties and uses of a new class of materials", *Material Science and Engineering*; 28(2000): 1-63
8. Shen, J.W., Chen, X.M. and Huang, W.Y. (2003). "Structure and Electrical Properties of Grafted Polypropylene/Graphite Nanocomposites Prepared by Solution Intercalation", *Journal of Applied Polymer Science*, 88: 1864–1869
9. Yasmin, A., Luo, J. and Daniel, I.M. (2006). Processing of Expanded Graphite Reinforced Polymer Nanocomposites, *Composites Science and Technology*, 66(9): 1182–1189.
10. Asma Yasmin, Isaac Daniel. 2004. "Mechanical and thermal properties of graphite platelet/ epoxy composites," *Polymer* 45 (24):8211-8219.
11. Peng Xiao, Min Xiao, Gong K. "Preparation of exfoliated graphite/ polystyrene composite by polymerization-filling technique" *Polymer*; 42 (2001) 4813-4816
12. Fukushima H., and Drzal L.T. 2004. "Graphite nanoplatelets as reinforcement for polymers: structural and electrical properties" Proceedings of 17th international conference on American Society for composites, September 9-11, 2004
13. ASTM Standard D-6110-06, "Standard Test Method for Determining the Charpy Impact Resistance of

- Notched Specimens of Plastics” *ASTM International* (2006)
14. ASTM Standard D-4065-01, “Standard Practice for Plastics: Dynamic Mechanical Properties: Determination and Report of Procedures”, *ASTM International* (2000)
 15. “Dynamic Mechanical Analyzer, Q Series™, Getting started guide” Revision F, Issued January 2004, TA Instruments, New Castle, Delaware
 16. “DMA theory and applications Training course” *March 2007*
 17. TA instruments website, “<http://www.tainstruments.com/pdf/DMA.pdf>” accessed on October 9, 2007, at 3:00 PM, pp 13
 18. Xu L.R., Sengupta S. 2005 “Interfacial stress transfer and property mismatch in discontinuous nanofiber/nanotube composite materials” *Journal of Nanoscience and Nanotechnology*; 5(4):620-626
 19. Xu L.R., Li L., Charles M.L., Kuai H. 2007 “Mechanical characterization of nanofiber-reinforced composite adhesives” *Journal of Nanoscience and Nanotechnology*; 7(7):2546-2548
 20. Mantena P.R., Mann R., Nori C. 2001. “Low-Velocity Impact Response and Dynamic Characteristics of Glass-Resin Composites” *Journal of Reinforced Plastics and Composites*; 20(6): 513-534

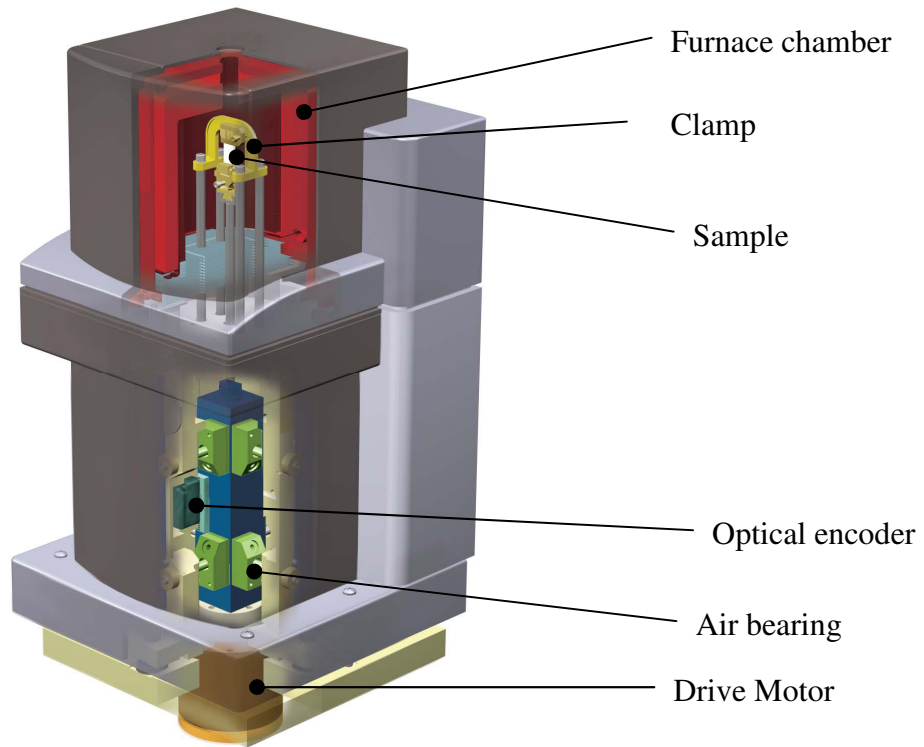


Figure 1: Schematic of TA instruments model Q800 DMA [17]

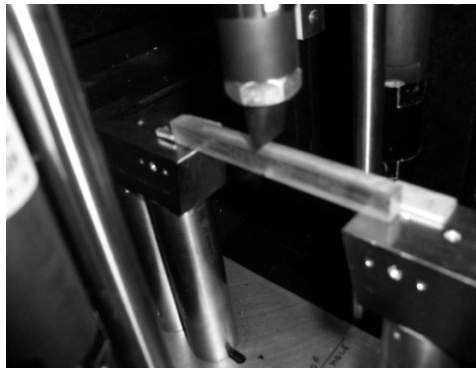


Figure 2. Nanoreinforced sample mounted in Dynatup 8250 impact test system

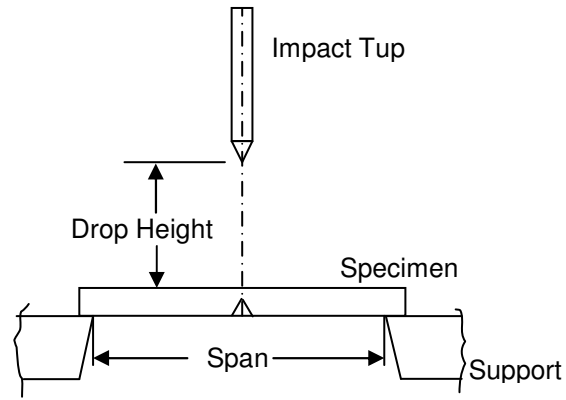


Figure 3. Schematic of the drop weight impact test

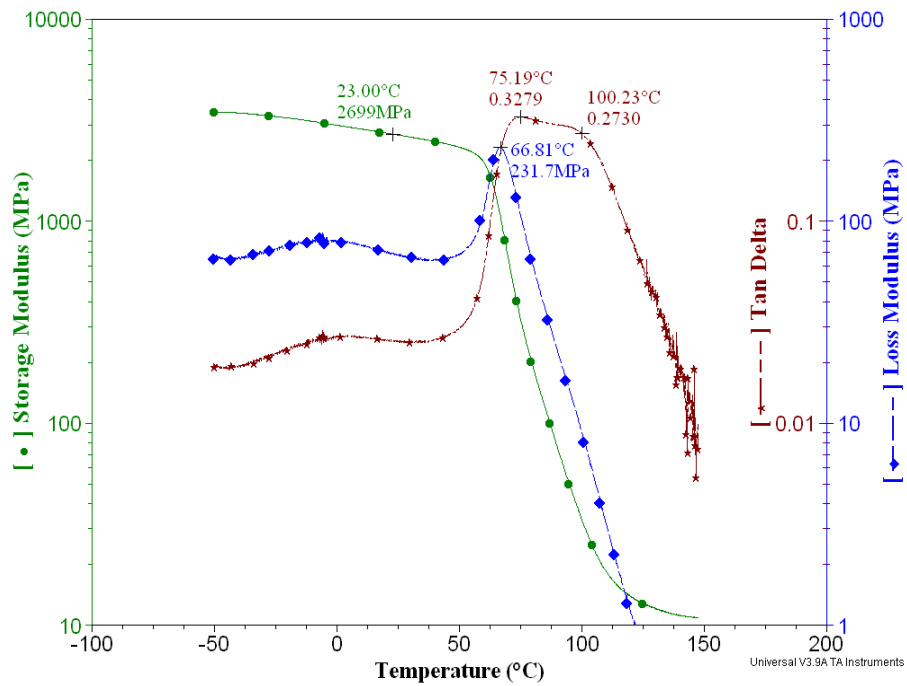


Figure 4. Typical dynamic modulus and damping for pure vinyl ester

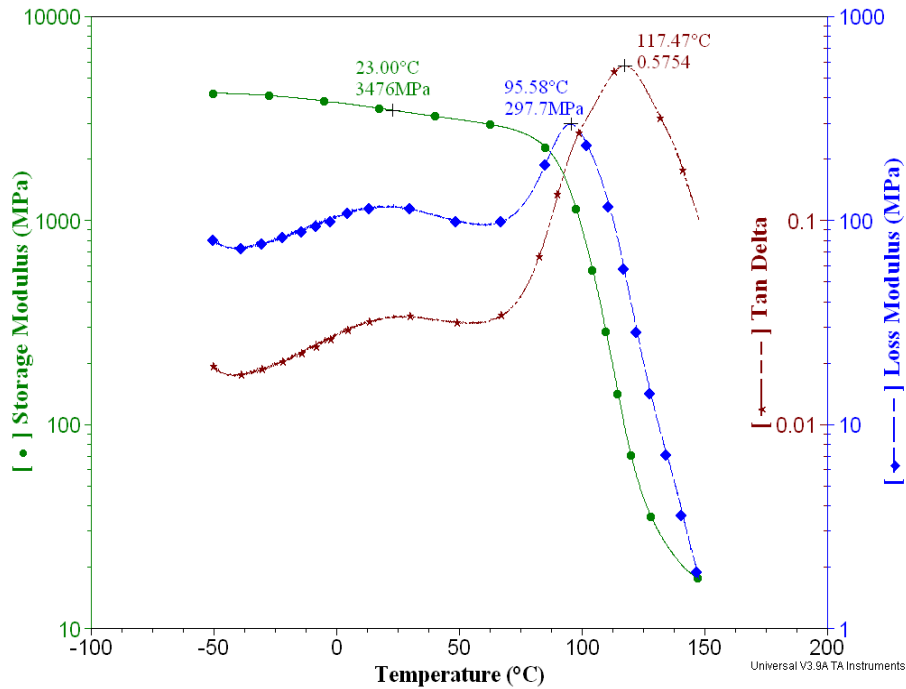


Figure 5. Typical dynamic modulus and damping for vinyl ester with 2.5 wt. percent graphite platelets

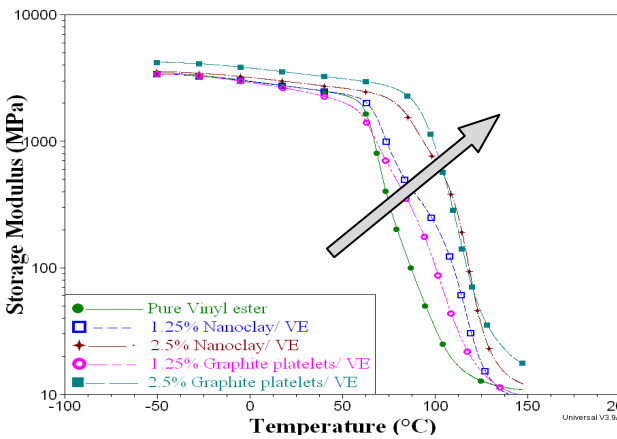


Figure 6(a): Storage modulus vs. temperature of vinyl ester nanocomposites at 23°C

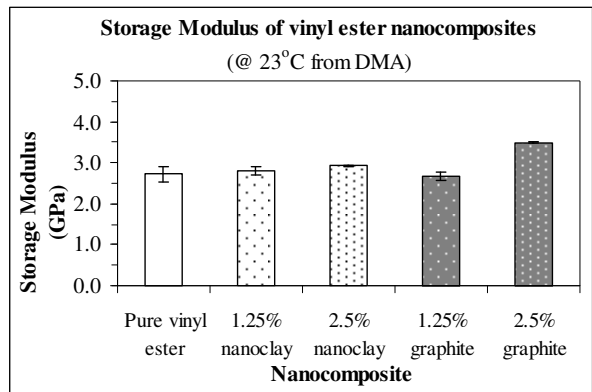


Figure 6(b): Storage modulus of vinyl ester nanocomposites at 23°C

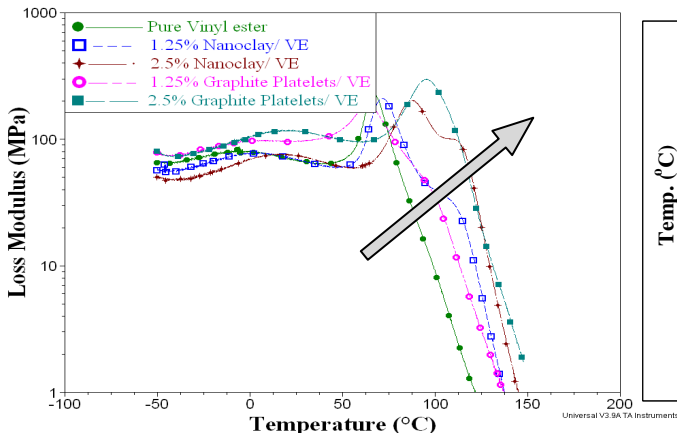


Figure 7(a): Loss modulus vs. temperature of vinyl ester nanocomposites at loss modulus peak

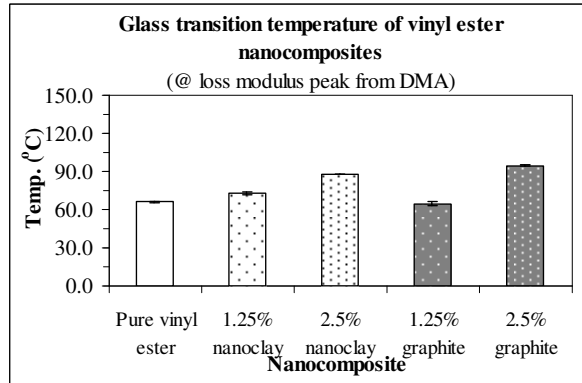


Figure 7(b): Glass transition temperature of vinyl ester nanocomposites at loss modulus peak

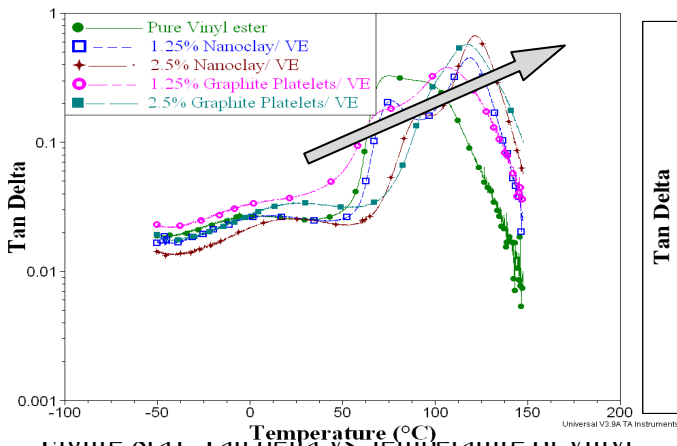


Figure 8(a): Tan Delta vs. temperature of vinyl ester nanocomposites

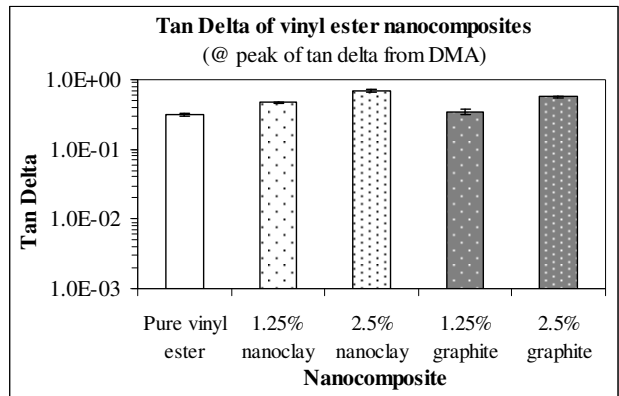


Figure 8(b): Loss factor of vinyl ester nanocomposites at peak of tan δ

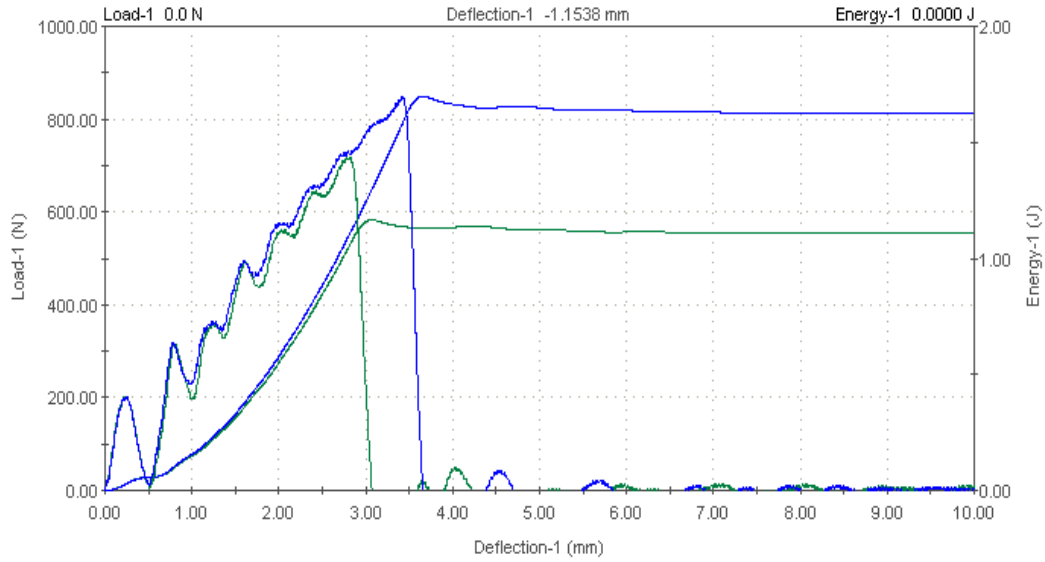


Figure 9: Typical impact load (and energy) vs. deflection for un-notched 2.5 wt percent graphite platelets reinforced vinyl ester specimens

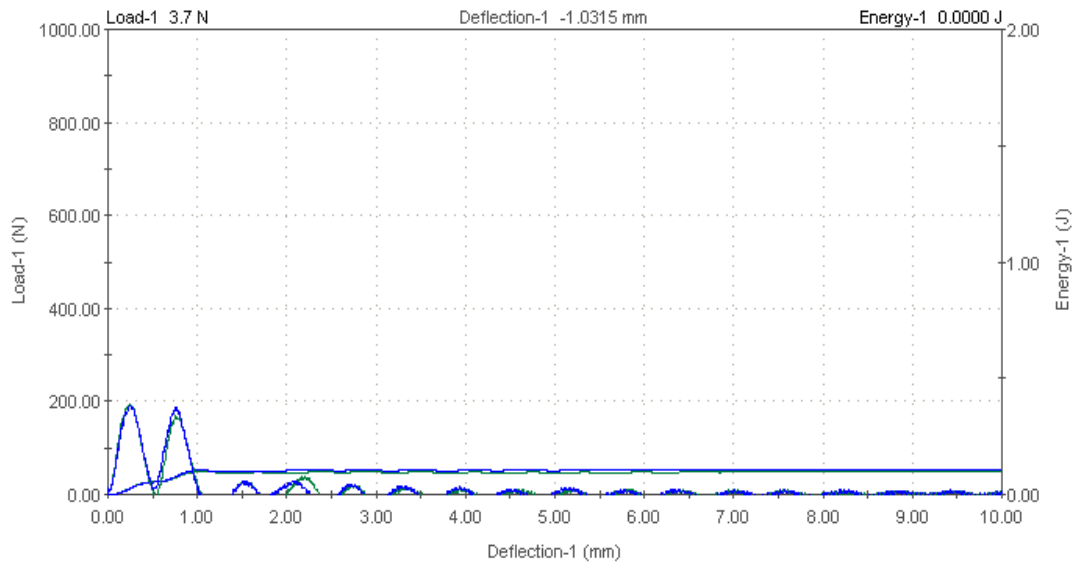


Figure 10: Typical impact load (and energy) vs. deflection for notched 2.5 wt percent graphite platelets reinforced vinyl ester specimens

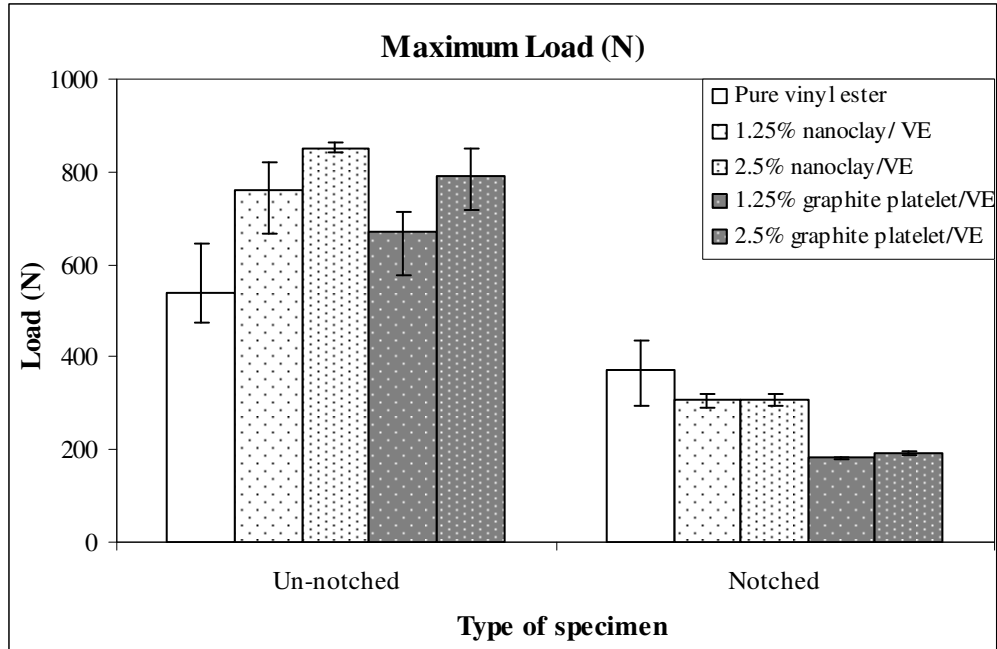


Figure 11: Maximum load comparison for notched and un-notched pure vinyl ester and nanoclay and graphite platelets reinforced composites

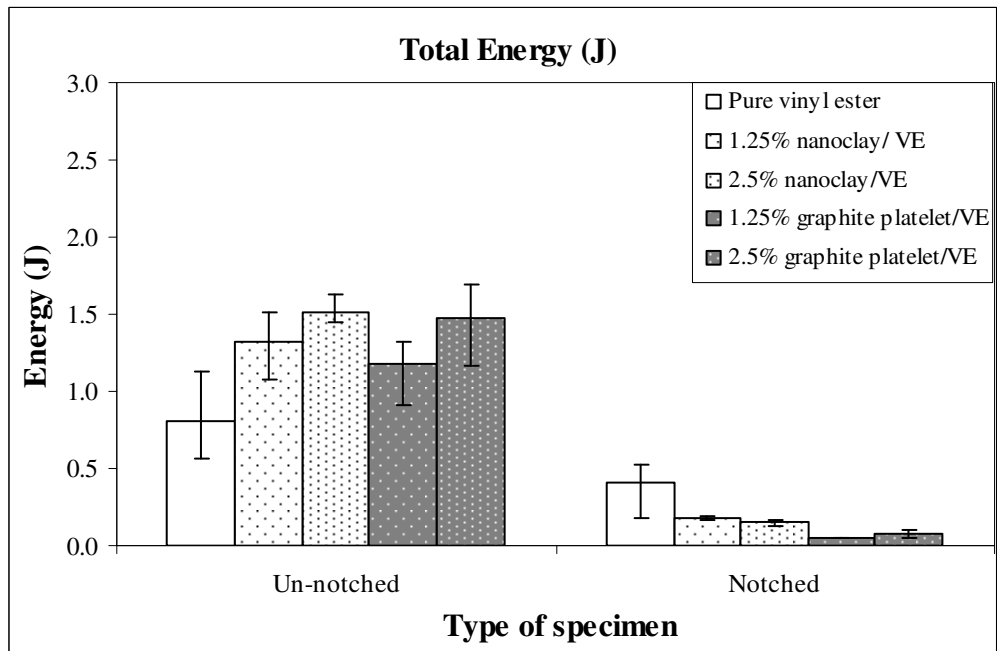


Figure 12: Total energy comparison for notched and un-notched pure vinyl ester and nanoclay and graphite platelets reinforced composites

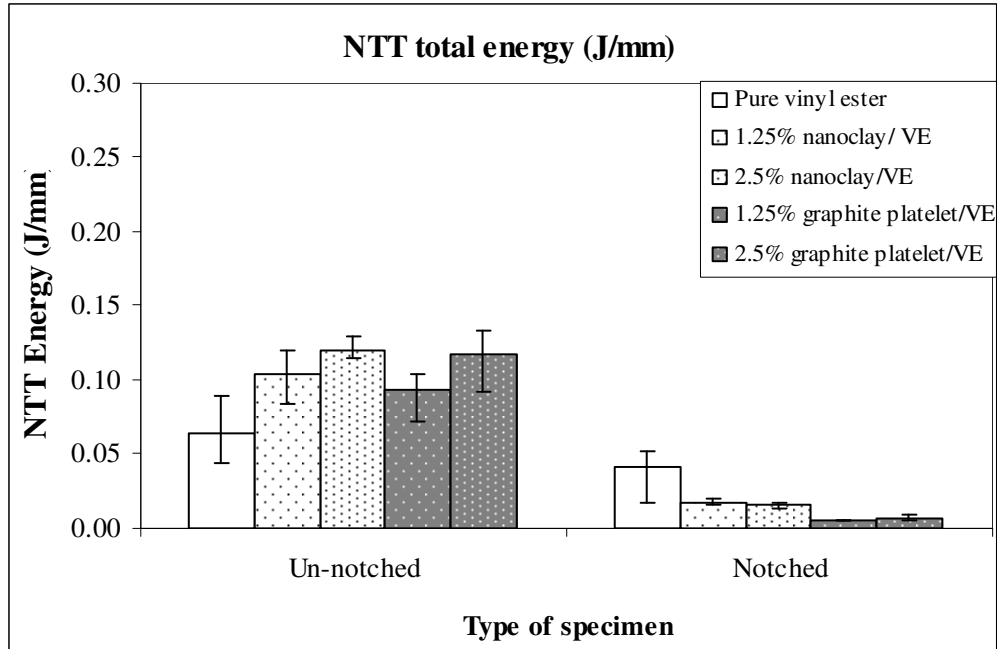


Figure 13: NTT total energy comparison for notched and un-notched pure vinyl ester and nanoclay and graphite platelets reinforced composites

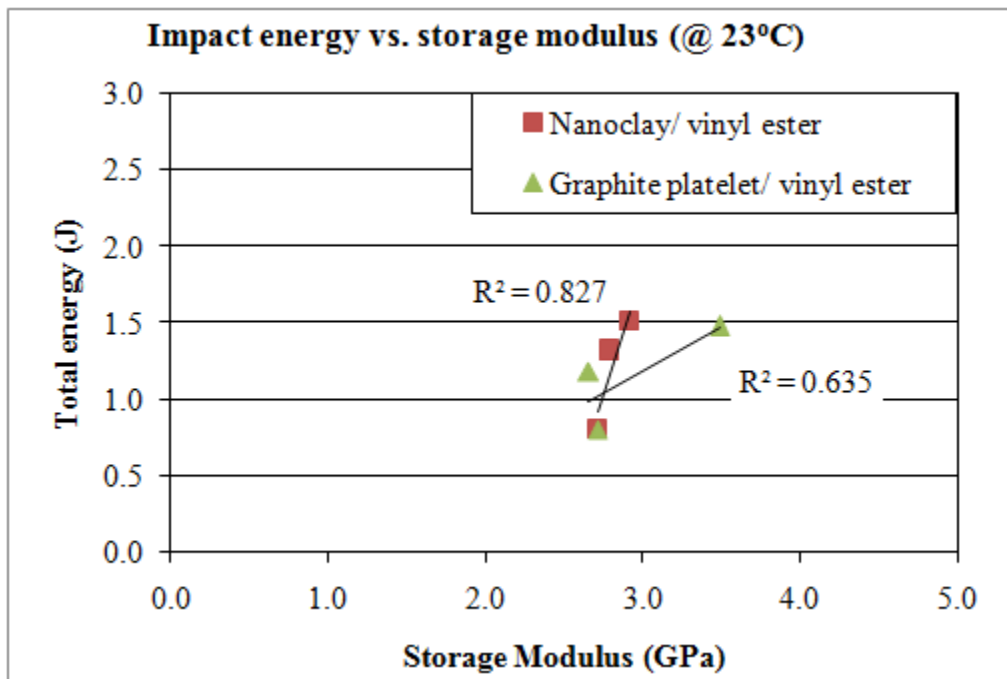


Figure 14: Total energy (from impact) vs. storage modulus (from DMA, at room temperature) for vinyl ester nanocomposites

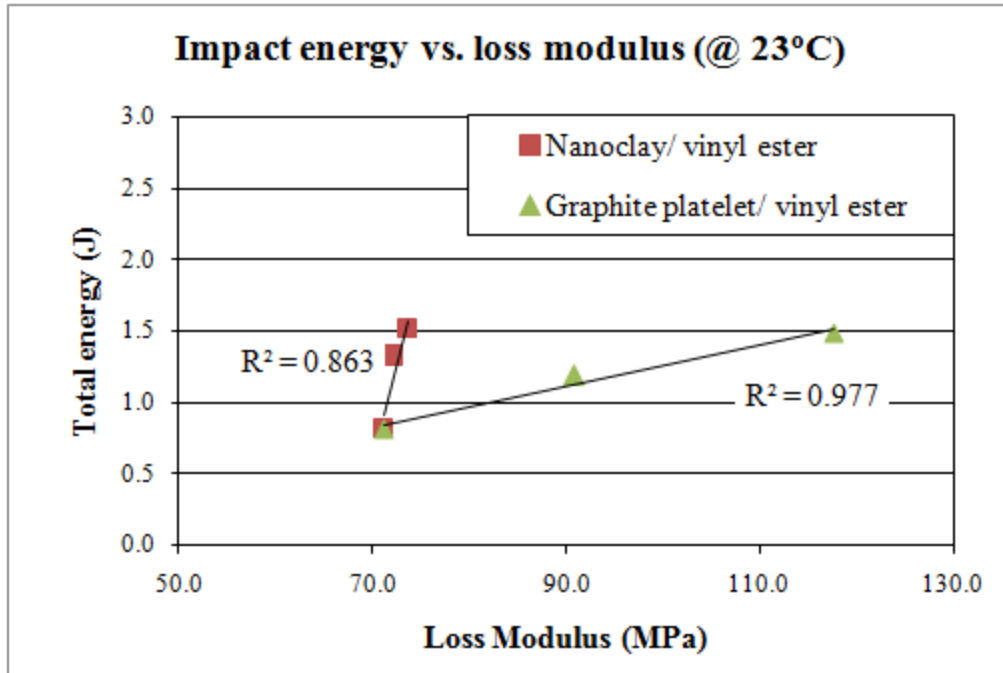


Figure 15: Total energy (from impact) vs. loss modulus (from DMA, at room temperature) for vinyl ester nanocomposites

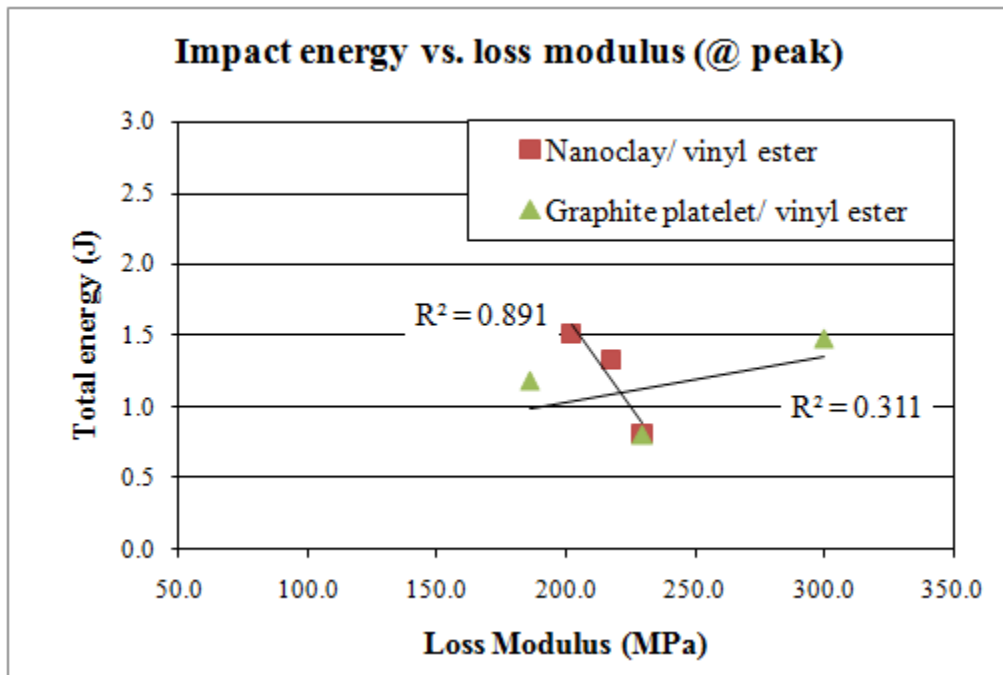


Figure 16: Total energy (from impact) vs. loss modulus (from DMA, at glass transition temperature) for vinyl ester nanocomposites

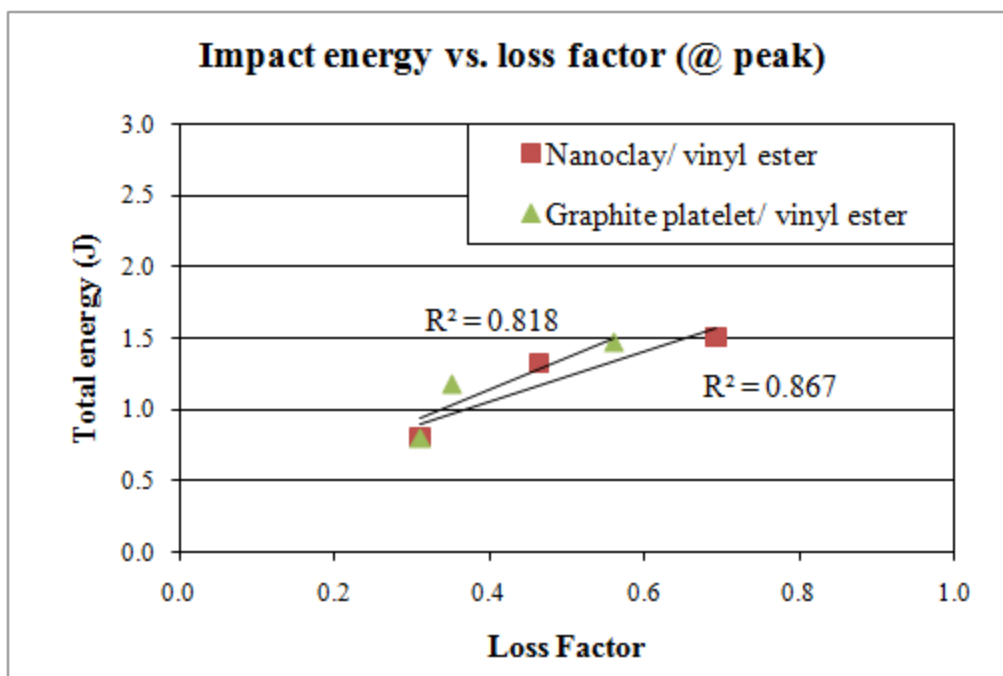


Figure 17: Total energy (from impact) vs. loss factor (from DMA, at tan delta peak) for vinyl ester nanocomposites

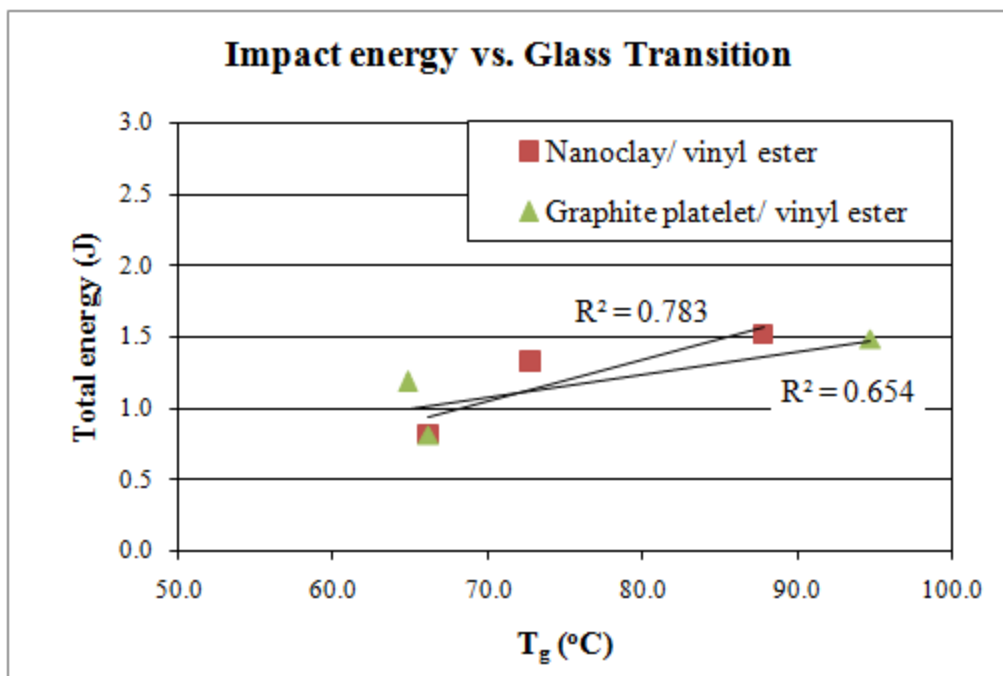


Figure 18: Total energy (from impact) vs. glass transition temperature (from DMA) for vinyl ester nanocomposites

